Exploring the Local Conformational Space of a Membrane Protein by Site-Directed Spin Labeling

David Stopar,[†] Janez Štrancar,[‡] Ruud B. Spruijt,[§] and Marcus A. Hemminga*[,§]

Biotechnical Faculty, University of Ljubljana, Večna pot 111, SI-1000 Ljubljana, Slovenia, Laboratory of Biophysics, Jožef Stefan Institute, Jamova 39, SI-1000 Ljubljana, Slovenia, and Laboratory of Biophysics, Wageningen University, Dreijenlaan 3, NL-6730 HA Wageningen, The Netherlands

Received April 26, 2005

Molecular modeling based on a hybrid evolutionary optimization and an information condensation algorithm, called GHOST, of spin label ESR spectra was applied to study the structure and dynamics of membrane proteins. The new method is capable of providing detailed molecular information about the conformational space of the spin-labeled segment of the protein in a membrane system. The method is applied to spin-labeled bacteriophage M13 major coat protein, which is used as a model membrane protein. Single cysteine mutants of the coat protein were labeled with nitroxide spin labels and incorporated in 1,2-dioleoyl-*sn*-glycero-3-phosphocholine (DOPC) bilayers. The new computational method allows us to monitor distributions of local spatial constraints and molecular mobility, in addition to information about the location of the protein in a membrane. Furthermore, the results suggest that different local conformations may coexist in the membrane protein. The knowledge of different local conformations may help us to better understand the function−structure relationship of membrane proteins.

INTRODUCTION

The function of a protein is directly related to its three-dimensional structure via specific interactions with its environment. The central importance of a structure−function relationship in molecular biology has driven rapid development of multidimensional NMR and X-ray crystallography that are capable of determining the atomic resolution of proteins in either solution or crystal environment, respectively. The development of structural methods for membrane proteins, however, has been much slower, and there are relatively few complete three-dimensional structures of membrane proteins available. A variety of structural problems poses significant challenges for both NMR and X-ray crystallography when applied to membrane proteins. Most notably are the large size of proteolipid complexes and the difficulty of crystal formation in a lipid environment, which have so far prevented their wider applicability.

In the past couple of years, several viable alternatives have been proposed. Among them is the method of site-directed spin labeling (SDSL), which has proven to be a powerful approach for the study of membrane protein structure and dynamics.[1−5] In this approach, site-specifically placed cysteine residues are used to introduce nitroxide radicals at a specific position in a protein sequence. ESR spectroscopy then yields structural information based on the mobility of the attached label, its accessibility to collisions with water or lipid soluble paramagnetic species, and structural constraints due to secondary or tertiary structure of the protein. In previous work using SDSL ESR, it was established that the backbone secondary and tertiary structure of membrane proteins could be determined from the periodic variations in the accessibility of different spin labels in a sequential set of spin-labeled proteins. It was also observed that the motional characteristics of the protein side chain, reflected in the ESR spectral line shape, correlates well with the predicted features of the protein fold. Spin labeling may provide only local information; however, conformational transitions that result in repacking along secondary or tertiary structural elements may provide information about the overall protein dynamics while performing a specific function. It is especially important that side-chain dynamics may provide a highly localized view of conformational changes triggering protein function. Also the application of SDSL ESR to the determination of structures and molecular mechanisms of a variety of water-soluble and membrane proteins has been shown to be very successful.[5−14]

Recently we have been exploring a new approach of analyzing ESR data from SDSL experiments,[15] showing that it is possible to enhance the information content arising from the ESR spectra. This approach is based on new computational methods to simulate ESR spectra of SDSL membrane proteins in a combination with hybrid evolutionary optimization followed by a GHOST condensation method. In particular by using this analysis, it becomes possible to determine the local conformation space of a spin-labeled protein.

In this work the major coat protein, a small transmembrane protein of bacteriophage M13 composed of 50 amino acid residues, is used to apply the new method of local conformational analysis to membrane proteins. Since structural and topological models of the major coat protein are known (for a recent review see ref 16), this protein is an excellent model

* Corresponding author phone: +31 317 482635 or +31 317 482044; fax: +31 317 482725; e-mail: marcus.hemminga@wur.nl; Web site: http://ntmf.mf.wau.nl/hemminga/. Corresponding author address: Laboratory of Biophysics, Wageningen University, P.O. Box 8128, 6700 ET Wageningen, The Netherlands. Office: Dreijenlaan 3, 6703 HA Wageningen.

[†] University of Ljubljana.

[‡] Jožef Stefan Institute.

[§] Wageningen University.

10.1021/ci0501490 CCC: $30.25
Published on Web 09/01/2005

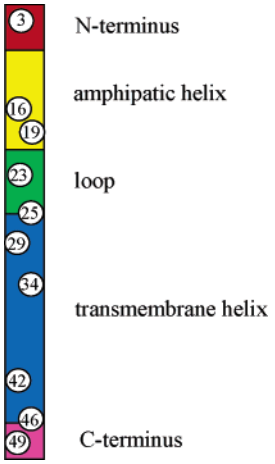

Figure 1. Location of the spin labels in the primary structure of the M13 major coat protein. The numbers refer to the amino acid residue position, which have been replaced for a cysteine in the various single-cysteine mutants of the protein.

system for the purpose of our work. By using site-directed mutagenesis cysteine residues were carefully placed at structurally significant parts of the protein (see Figure 1). Single cysteine mutants were labeled with nitroxide spin labels and incorporated in 1,2-dioleoyl-*sn*-glycero-3-phosphocholine (DOPC) bilayers. The new computational method allowed us to monitor distributions of local spatial constraints, molecular mobility, interaction with paramagnetic oxygen, and the determination of polarity gradients along the protein sequence in the lipid membrane environment. Furthermore, the results suggest that different local conformations may coexist in the membrane protein that may enable it an easy transition to the functional structure.

MATERIALS AND METHODS

Sample Preparation. Site-specific cysteine mutants of bacteriophage M13 major coat protein were prepared, purified, and labeled with 3-maleimido proxyl spin label (Aldrich) as described previously.[17,18] The cysteine residues were introduced by site-directed mutagenesis into different domains of the protein, as shown in Figure 1. Labeled mutants were reconstituted into DOPC bilayers at a lipid-to-protein ratio of 100 (Avanti Polar Lipids) as reported earlier.[11,19] The proteoliposomes were concentrated as described before, using lyophilization and subsequent rehydration, and were collected by high-speed centrifugation.

ESR Spectroscopy. Samples of reconstituted spin-labeled mutants in DOPC were filled up to 5 mm in 50 μL glass capillaries that were accommodated within standard 4-mm diameter quartz tubes. ESR spectra were recorded at room temperature on a Bruker ESP 300E ESR spectrometer equipped with a 108TMH/9103 microwave cavity. The ESR settings were as follows: 6.38 mW microwave power, 1 G modulation amplitude, 40 ms time constant, 80 s scan time, 100 G scan width, and 3389 G center field.[5] Up to 20 spectra were collected to improve the signal-to-noise ratio.

ESR Spectral Simulation. Generally, to describe the ESR spectra of spin labels, the stochastic Liouville equation should be used.[20−22] However, under physiological conditions the majority of the local rotational motions is fast with respect to the ESR time scale, and therefore a fast motional approximation can be applied, gaining a factor of 100 in the computation time needed for spectral simulations. Application of multiple rotational correlation times together with multiple parameters that define the anisotropy of the rotational motions, i.e., wobble angles, usually gives rise to numerically ill-posed optimization problems. To avoid this, we decided to use a single rotational correlation time that empirically describes the rate of the rotational motion of the spin label in addition to two wobble angles that define the anisotropy of the rotational motions.[15]

The basic principles of the ESR spectral simulations have been discussed elsewhere.[15,23] Here we emphasize the physical background of the spectral parameters that were involved in the calculation. Two parameters, ϑ and φ, were used to describe the partial averaging of the rotational motion while averaging the magnetic properties of spin Hamiltonian for spin probes directed at every allowed orientation with respect to the external magnetic field. The restrictions of the rotational motions were described by an opening cone angle ϑ (that defines the maximal tilt angle) and a cone asymmetry angle φ (that describes the maximal restriction of rotation). The traces of the magnetic interaction tensors **g** and **A** were linearly corrected with the parameters p_A that describes the effects of polarity and prot that counts for proticity.[24] However, in the case of X-band spectral simulations, the prot parameter is poorly resolved—the relative error is around 20%. Therefore the prot parameter will be neglected in our further discussion. When calculating the convolution of the magnetic field distribution and the basic line shape, two line width parameters, τ_c and W, were applied. The Lorentzian line was defined in the motional narrowing approximation with a single (effective) rotational correlation time τ_c.[25] To describe the additional broadening of the spectral line, a constant W was applied. This parameter arises primarily from unresolved hydrogen superhyperfine interactions and contributions from paramagnetic impurities (e.g. oxygen), external magnetic field inhomogeneities, field modulation effects, and intermolecular spin−spin interaction.

To take into account a superposition of motional and polarity patterns, this basic set of parameters ϑ, φ, τ_c, W, and p_A is expanded for the number of spectral components N_c. In addition there are N_c-1 weights of these spectral components. Altogether, there are $7N_c-1$ spectral parameters, which have to be resolved by the optimization routine. The resolution limit of spin label ESR is around 30 parameters. This is based on the criteria of average ESR line width and maximal hyperfine splitting. Therefore a maximum of 4 spectral components with 7 parameters can be resolved from the ESR spectra.

Optimization and Solution Condensation. To guide the optimization a common fitness function is introduced, the reduced χ^2, which is the sum of the squared residuals between the experimental and simulated spectral points divided by the squared standard deviation of the experimental points and by the number of points in the experimental spectrum (in our case 1024). Due to the complex search space of spectral parameters (28 parameters), hybrid evolutionary optimization (HEO) was used as an optimization method.[23] Based on our previous work with hybrid evolution multirun optimization procedures, it was possible to extract discrete groups of spectral parameters without predefining the number of groups in advance.[15] For multirun HEO optimization 200 runs were applied in our case. Furthermore, the same

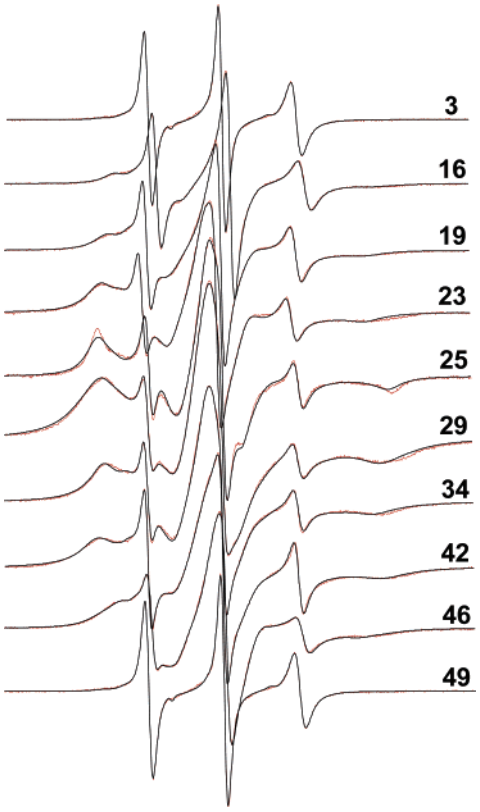

Figure 2. ESR spectra of 3-maleimidoproxyl site-directed spin-labeled M13 mutant coat protein at various positions reconstituted in DOPC multilamellar vesicles at a lipid-to-protein ratio of 100 in 150 mM NaCl, 10 mM Tris (pH 8.0), and 0.2 mM EDTA at room temperature (black line). Simulated spectra (red lines) were fitted to the experimental ESR spectra using a hybrid evolution optimization (HEO) optimization in combination with a GHOST condensation. Spectral line heights are normalized to the same central line height.

methodology, although with a reduced quality, can be used to characterize an even quasicontinuous distribution of spectral parameters. Although only the best-fit parameter sets of each run were extracted from the multiple HEO runs, a large amount of information needs to be condensed. For this purpose we used a so-called GHOST condensation algorithm[15] that filters the solutions according to their goodness of fit, solution density in the parameter space and performs group recognition by a slicing method. All the HEO and GHOST parameters were applied in the same way as described previously.[15]

RESULTS

The ESR spectra of different spin-labeled mutants of M13 major coat protein reconstituted in DOPC are given in Figure 2. The protein is a monotopic membrane protein, i.e., it traverses the membrane only once.[26,27] The ESR spectra of the spin-labeled protein can be classified into three distinct groups: (i) water-accessible spin-labeled amino acid residues at both ends of the protein; (ii) membrane-incorporated; and (iii) interfacial located spin-labeled amino acid residues. It can be seen that spectra of the spin-labeled mutants located at the opposite ends of the protein have a similar line shape, as would be expected for a monotopic protein passing through a membrane. For example, the spectrum of G3C in the N-terminal part of the protein has a similar isotropic appearance as the spectrum of the A49C mutant in the C-terminal part of the protein. The spectrum of the spin-labeled mutant T19C has a similar composite appearance as the spin-labeled mutant T46C located at the lipid−water interface. Spin-labeled mutants that are supposed to be located in the membrane interior, i.e., A25C and V29C, were strongly immobilized as inferred from the outer hyperfine splitting $2A_{zz}$, which were 62 and 60 G, respectively. In all spectra a small isotropic additional spectral component with a hyperfine splitting of 16 G can be observed.

All the ESR spectra shown in Figure 2 were simulated with a model of asymmetric motional restriction and characterized via a hybrid evolution optimization method.[15] In all cases the quality of the simulated spectra was excellent. From the simulations various spectral parameters (i.e. ϑ, φ, τ_c, W, and p_A) were obtained. The spectral parameters obtained from a single optimization run represent one point in the solution space. When 200 of such solutions were put together, several groups of solutions were identified. The GHOST condensation method was then applied to discriminate between the groups of solutions and describe their center of mass and second moment by appropriate values of the spectral parameters. The results for different spin-labeled mutants are shown in Figure 3. The plots in Figure 3 represent the effective local space and shape within which the spin label attached to the protein can move. Apart from the two water accessible spin-labeled amino acid residues at positions 3 and 49, all other spin-labeled amino acid residues had at least three groups of spectral parameter solutions. One group of the solutions (dark blue) was always the same and did not depend on the amino acid position. The spin probes contributing to this solution were not restricted in their rotational motions, because they could move in a completely open symmetrical cone. Slightly more restricted was the component indicated in red. The restriction was more pronounced for spin-labeled sites located in the transmembrane helix domain (i.e. A25C). The relative contribution of both blue and red components varied between 8 and 36% of the total ESR intensity, depending on the amino acid residue. Due to motional characteristics, and the relative independence on amino acid position, these two fractions were assigned to a nonspecific spin labeling of the protein. It is known that under the experimental conditions applied for labeling cysteines also the ϵ-amino group of lysines as well as N-terminal amino groups can react although to a smaller extent, because the reactivity is less (data of the labeled wild-type protein, lacking any cysteines, not shown). Lysines have a long side chain, so that spin labels that will be attached at the reactive group at the end of the side chain will show a large extent of motion. However, this motion will be reduced as compared to a spin label attached to the N-terminal NH_2 group.

The largest group indicated with a green color in Figure 3 contributed approximately 70% to the total ESR intensity. This group of solutions was strongly dependent on the position of the spin label. Both in terms of restrictions and asymmetry of the local environment this group is consistent with a transmembrane topology of the protein. In the interface region the opening of the cone angle was in the range between 0.5 and 0.8 rad for the different spin-labeled mutants, while for the spin labels located in the transmembrane helix domain the local restriction was more severe,

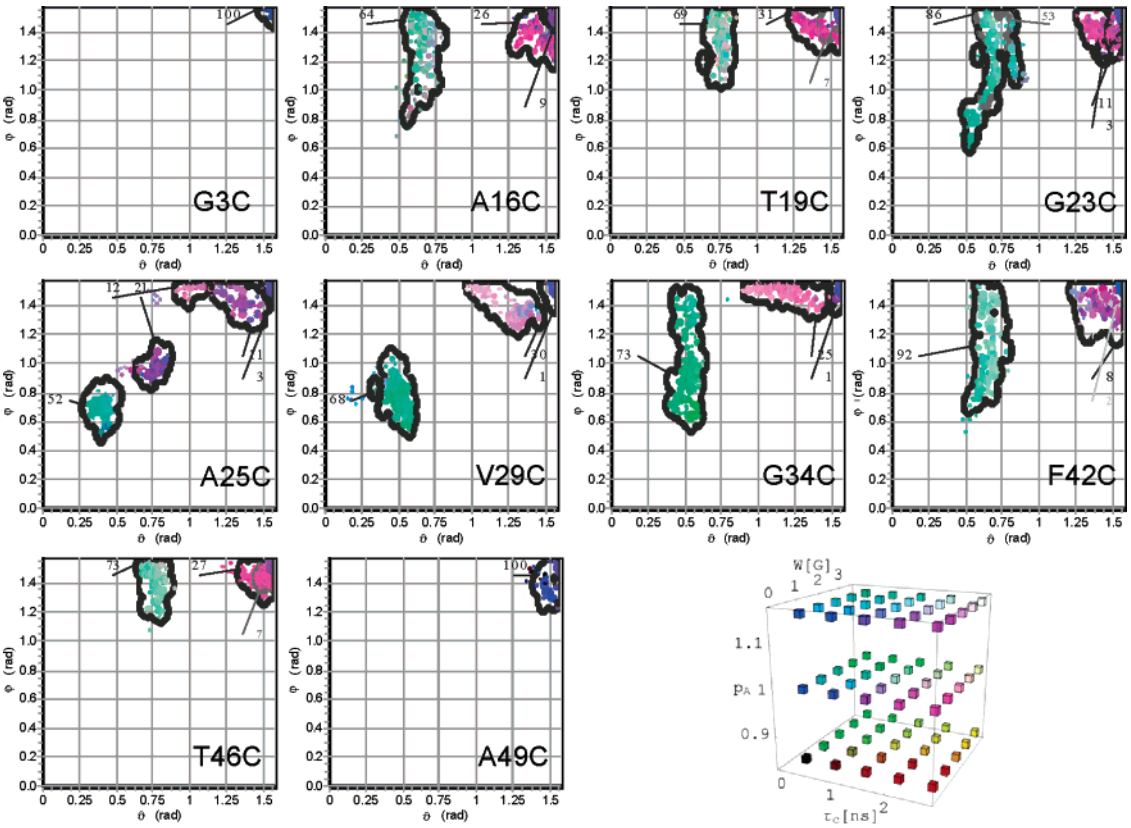

Figure 3. GHOST condensation of different spin-labeled M13 coat protein mutants reconstituted in DOPC vesicles. The parameter ϑ is the cone angle within the spin probe can move, and parameter φ describes the asymmetry of the cone. The relative fractions of a group of solutions for the two spectral parameters are indicated for each spin-labeled mutant with a larger font, in addition to small gray letters that indicate the fraction of the subgroups, if they exist. The RGB (red, green, and blue) color of the solutions codes for the relative values of τ_c, W, and p_A in their definition intervals {0−3 ns}, {0−4 G}, and {0.8−1.2}, respectively, as given by the color legend.[15]

being in the range between 0.25 and 0.6 rad. The position 25 is interesting because two restricted solutions were found with different τ_c, W, and p_A spectral characteristics. In the remaining part of the paper, we will focus on the analysis of the green-colored component in Figure 3.

In addition to the local spatial constraints, the spectral simulations provided information about the variation of the rotational correlation time at different locations along the protein sequence. As shown in Figure 4, the rotational correlation time for the spin labels at the extreme ends of the protein is approximately 0.5 ns (G3C and A49C). However, there is a significant increase in τ_c at positions at the N-terminal edge of the loop region (i.e. A16C and T19C, see Figure 1) and the C-terminal edge of the transmembrane helix (i.e. F42C and T46C). Positions within the transmembrane helix (i.e. 34) had a lower value of τ_c again.

The dependence of the additional spectral line broadening, W, on the amino acid position is given in Figure 5. An additional line broadening in the ESR line shape may arise from several different sources: spin−spin dipolar interactions due to protein aggregation, presence of other paramagnetic species, magnetic field modulation, and magnetic field inhomogeneities. We can neglect the last two in our case. As the motion of the spin probe is restricted and therefore anisotropic, the broadening could partially result from dipolar interaction due to protein aggregation. However, an extensive aggregation of the M13 major coat protein under the conditions used in this study can be ruled out.[28] On the other hand, in progressive saturation ESR experiment molecular oxygen and Ni^{2+} ions as paramagnetic relaxation agents were

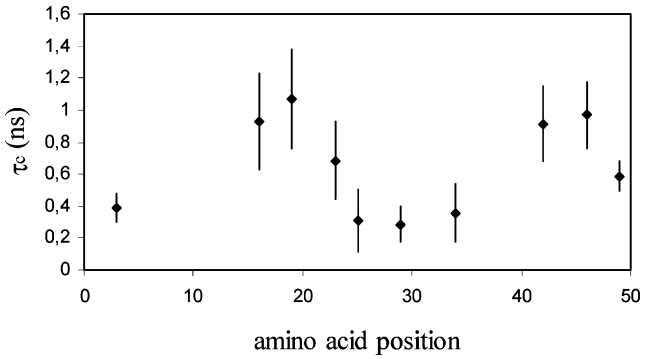

Figure 4. Dependence of average rotational correlation time τ_c of the major spectral component on mutant amino acid position obtained from ESR spectral simulation of spin-labeled M13 coat protein when reconstituted into DOPC bilayers. The center of mass (data point) and the corresponding second moments (error bars) of τ_c are indicated. The ESR spectra were recorded at room-temperature well above the gel-to-liquid crystalline phase transition temperature of DOPC.

used to determine the dependence of spin label position of the relaxation enhancement by oxygen and Ni^{2+}.[13] Therefore the most obvious candidates for additional line broadening are paramagnetic oxygen molecules that are known to dissolve preferentially in the hydrophobic phase.[29,30] It was also shown in the literature that one can measure oxygen variation by saturation ESR techniques and line width measurements.[13,31] Consistently a relatively low additional spectral line broadening was observed for the water located G3C and A49C spin-labeled sites in the N and C-terminal

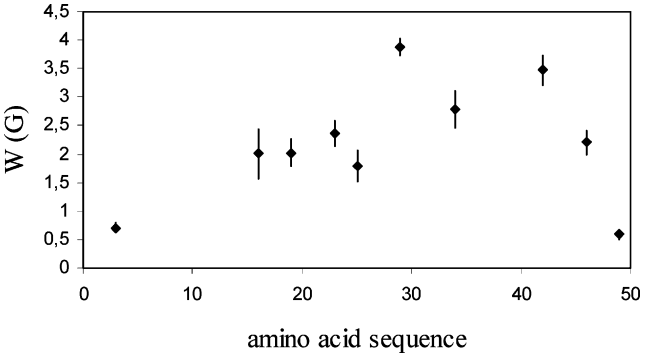

Figure 5. The dependence of the average ESR additional spectral line broadening, *W*, obtained from ESR spectral simulation on the major coat protein amino acid position. The M13 major coat protein was reconstituted into DOPC bilayers. The center of mass and corresponding second moment of *W* are indicated. The ESR spectra were recorded at room-temperature well above the gel-to-liquid crystalline phase transition temperature of DOPC.

part of the protein, respectively. Starting at positions near the edges of the transmembrane protein part, *W* increased. The accessibility of the spin-labeled sites for oxygen was approximately 5-fold higher in the transmembrane part of the protein as compared to the aqueous environment. From the profile in Figure 5 it is clear that protein is not symmetrically located in the lipid bilayer.

DISCUSSION

Site-directed spin-label ESR is used in this paper in a combination with simulation and GHOST computational condensation to resolve local conformational states of the M13 major coat protein in a membrane environment. Ten spin labeled mutants that were selected to be regularly spaced along the primary sequence of the protein were reconstituted into DOPC bilayers. The structure and topology of the major coat protein in the lipid bilayers has been described already previously and can be used as a reference for the present work.[11,13,18,32−38] Also in our previous work the effect of replacing amino acid with cysteine has been checked. With respect to the membrane-bound properties, the analyses of the structural and aggregational properties of the mutants were indistinguishable from the wild-type M13 major coat protein.[5,18] In this work we have demonstrated that our new computational approach of ESR analysis is capable of providing detailed local molecular information in terms of protein structure, dynamics, and membrane location.

Although four spectral components were used to fit the ESR data, it can be seen from the GHOSTs (Figure 3), that our approach resolves a complex distribution of spectral parameters. For example, in the case of the highly isotropic G3C or A49C spin-labeled mutants, the same four-component model was used as for the other mutants, but only one well-defined group of spectral parameters appeared. This is what one would expect in the absence of protein secondary structural elements in a well-defined isotropic local environment. In the case of other spin-labeled mutants in the amphipathic or transmembrane part of the protein, there were several groups of solutions. The observed distribution of spectral parameters should not come as a surprise when the actual complexity of the protein and its numerous molecular interactions with the membrane environment are taken into account.[16] Therefore the ESR spectra are very likely composed of several superimposed spectral components, each representing a distribution of spectral parameters around a center of mass. However, these spectral features may not be resolved without spectral simulation and other computational methods of data analyses.[15] The advantage of our analysis is that there is no need to define the complexity of the solution space in advance.

Although several groups of ESR spectral parameters were observed, only the green-colored group of solutions in Figure 3 shows a significant effect on amino acid position, a situation compatible with the transmembrane topology of the protein. The other groups, which represent minor components in the total ESR spectral intensity, were unrestricted in mobility and show little dependence on the amino acid position and were assigned to nonspecific labeling of the protein. Since more information about protein structure, dynamics, and location in the lipid bilayer is present in the green-colored component, we will concentrate on this solution in the following discussion.

From the different spectral parameters obtained (see Figures 3−5) it can be seen that both termini of the protein are located in an aqueous environment. There is also little doubt about the membrane embedment of the part of the protein between position 25 and 42, as deduced from the more restricted space in which the spin label can move (see ϑ and φ), the low correlation rotational time ($\tau_c \sim 0.3$ ns), and the high accessibility to oxygen ($W \sim 3.5$ G). Such a protein topology is in very good agreement with the structural and topological models of the major coat protein in DOPC bilayers.[36,38−40] The relaxation enhancement profile for oxygen (Figure 5) exhibits a strong asymmetric distribution across the membrane toward the C-terminus. Additionally, the rotational correlation time profile of the spin-labeled residues (Figure 4) is highly asymmetric. This is related to the domain structure of the protein (see Figure 1). It has been suggested earlier that the membrane-bound form of the protein is composed of two helices: a transmembrane helix and an amphipathic helix that are oriented perpendicular to each other.[36,39,41] From the recent information, however, it follows that the protein in DOPC bilayers forms a continuous banana-shaped α-helix.[38] To adapt to the thickness of the lipid bilayer the transmembrane domain of the protein makes a tilt of about 25° relative to the normal to the lipid bilayer.[42,43] This would bring the spin-labeled sites in the amphipathic helix close to the lipid−water interface. The low-resolution data given in Figures 4 and 5 suggest that amphipathic helix is located close to the water−lipid interface.

Figure 3 describes the GHOST condensation analysis of different spin-labeled M13 coat protein mutants reconstituted into DOPC vesicles. The groups of solutions contain both a computational error and a distribution of different solutions in space and time of the spin label attached to the protein. If there would be only errors contributing to the GHOSTs in Figure 3, then we would expect a Gaussian distribution of errors around a center of mass. However, most solutions are not isotropic. This especially applies to sites on the transmembrane protein domain represented by the green-colored component in Figure 3. This suggests that there is also a distribution of different solutions around a center of mass. In fact, this relates to different local conformations for a single labeled site on the protein. Therefore, the data

presented in Figure 3 demonstrate that protein locally exists in a variety of different conformations. On the ESR time scale we only see a frozen picture, which means that the spin label is observed in different proteins frozen in different local conformations (i.e. different cones). However, there is no a priori reason that the spin label cannot go through all these local conformations. Since the different cones form the same group of spectral solutions given in the GHOST representation (see Figure 3), it is reasonable to expect that the spin label may have access to all of them. If this would not be the case, we would see an average local conformation and not a distribution. Based on the ESR time scale, it can be estimated that the time to go from one local conformation to the other local conformation is at least 3 ns. This relatively slow time scale may be related to the fact that a change of the local conformation probably involves also changing neighboring sites, which costs energy and time. Nevertheless, this transition time would still give the protein a great deal of local flexibility and could probably facilitate a structural rearrangement of the major coat protein during incorporation in the membrane and assembly in the new virus particle.

The work presented in this paper establishes a new basis for the interpretation of ESR line shapes in terms of a detailed local conformational structure of membrane proteins. In addition, it sets the stage for a wider range of applications of site-directed spin-labeling to problems related to the determination of the structure of membrane proteins, protein folding pathways, protein topology, protein−lipid interactions, hydrophobic mismatch, and detection of function-related conformational changes of membrane proteins.

Abbreviations used: SDSL, site-directed spin labeling; GHOST, information condensation algorithm; DOPC, 1,2-dioleoyl-*sn*-glycero-3-phosphocholine, HEO, hybrid evolutionary optimization.

ACKNOWLEDGMENT

This work was supported by contract no. QLG-CT-2000-01801 of the European Commission.

REFERENCES AND NOTES

(1) Fajer, P. G. Electron spin resonance spectroscopy labeling in peptide and protein analysis. In *Encyclopedia of Analytical Chemistry*; Mayers, R. A., Ed.; John Wiley & Sons Ltd.: Chichester, 2000.

(2) Hubbell, W. L.; Altenbach, C. Investigation of structure and dynamics in membrane proteins using site-directed spin labeling. *Curr. Opin. Struct. Biol.* **1994**, *4*, 566−573.

(3) Hubbell, W. L.; Mchaourab, H. S.; Altenbach, C.; Lietzow, M. A. Watching proteins move using site-directed spin labeling. *Structure* **1996**, *4*, 779−783.

(4) Hustedt, E. J.; Beth, A. H. Nitroxide spin−spin interactions: applications to protein structure and dynamics. *Annu. Rev. Biophys. Biomol. Struct.* **1999**, *28*, 129−153.

(5) Stopar, D.; Spruijt, R. B.; Wolfs, C. J. A. M.; Hemminga, M. A. Local dynamics of the M13 major coat protein in different membrane-mimicking systems. *Biochemistry* **1996**, *35*, 15467−15473.

(6) Berengian, A. R.; Parfenova, M.; Mchaourab, H. S. Site-directed spin labeling study of subunit Interactions in the α-Crystallin domain of small heat-shock proteins. *J. Biol. Chem.* **1999**, *274*, 6305−6314.

(7) Columbus, L.; Kalai, T.; Jeko, J.; Hideg, K.; Hubbell, W. L. Molecular motion of spin labeled side chains in α-helices: analysis by variation of side chain structure. *Biochemistry* **2001**, *40*, 3828−3846.

(8) Klug, C. S.; Su, W.; Feix, J. B. Mapping of the residues involved in a proposed *β*-strand located in the Ferric Enterobactin Receptor FepA using site-directed spin labeling. *Biochemistry* **1997**, *36*, 13027−13033.

(9) Liu, Y.-S.; Sompornpisut, P.; Perozo, E. Structure of the KcsA channel intracellular gate in the open state. *Nature Struct. Biol.* **2001**, *8*, 883−887.

(10) Mchaourab, H. S.; Oh, K. J.; Fang, C. J.; Hubbell, W. L. Conformation of T4 lysozyme in solution. Hinge-bending motion and the substrate-induced conformational transition studied by site-directed spin labeling. *Biochemistry* **1997**, *36*, 307−16.

(11) Meijer, A. B.; Spruijt, R. B.; Wolfs, C. J. A. M.; Hemminga, M. A. Configurations of the N-terminal amphipathic domain of the membrane-bound M13 major coat protein. *Biochemistry* **2001**, *40*, 5081−5086.

(12) Perozo, E.; Cortes, M. D.; Sompornpisut, P.; Kloda, A.; Martinac, B. Open channel structure of MsdL and the gating mechanism of mechanosensitive channels. *Nature* **2002**, *418*, 942−948.

(13) Stopar, D.; Jansen, K. A. J.; Páli, T.; Marsh, D.; Hemminga, M. A. Membrane location of spin-labeled M13 major coat protein mutants determined by paramagnetic relaxation agents. *Biochemistry* **1997**, *36*, 8261−8268.

(14) Wegener, A. A.; Klare, J. P.; Engelhard, M.; Steinhoff, H.-J. Structural insights into early steps of receptor-transducer signal transfer in archaeal phototaxis. *EMBO J.* **2001**, *20*, 5312−5319.

(15) Štrancar, J.; Koklic, T.; Arsov, Z.; Filipic, B.; Stopar, D.; Hemminga, M. A. Spin label EPR-based characterization of biosystem complexity. *J. Chem. Inf. Model.* **2005**, *45*, 394−406.

(16) Stopar, D.; Spruijt, R. B.; Wolfs, C. J.; Hemminga, M. A. Protein−lipid interactions of bacteriophage M13 major coat protein. *Biochim. Biophys. Acta* **2003**, *1611*, 5−15.

(17) Meijer, A. B.; Spruijt, R. B.; Wolfs, C. J. A. M.; Hemminga, M. A. Membrane-anchoring interactions of M13 major coat protein. *Biochemistry* **2001**, *40*, 8815−8820.

(18) Spruijt, R. B.; Meijer, A. B.; Wolfs, C. J. A. M.; Hemminga, M. A., Localization and rearrangement modulation of the N-terminal arm of the membrane-bound major coat protein of bacteriophage M13. *Biochim. Biophys. Acta* **2000**, *1509*, 311−323.

(19) Spruijt, R. B.; Wolfs, C. J. A. M.; Hemminga, M. A. Aggregation-related conformational change of membrane-associated coat protein of bacteriophage M13. *Biochemistry* **1989**, *28*, 9158−9165.

(20) Budil, D. E.; Lee, S.; Saxena, S.; Freed, J. H. Nonlinear-least-squares analysis of slow-motion EPR spectra in one and two dimensions using a modified Levenberg−Marquardt algorithm. *J. Magn. Reson.* **1996**, *120*, 155−189.

(21) Robinson, B. T., H.; Beth, A.; Fayer, P.; Dalton, L. R. The phenomenon of magnetic resonance: Theoretical considerations. In *Advanced EPR Studies of Biological Systems*; Dalton, L., Ed.; CRC Press: Boca Raton, FL, 1985; pp 11−110.

(22) Schneider, D. J.; Freed, J. H. Calculating slow motional magnetic resonance spectra: a user's guide. In *Biological Magnetic Resonance: Spin Labeling, Theory and Applications*; Berliner, L. J., Reuben, J., Eds.; Plenum Press: New York, 1989; pp 1−76.

(23) Filipic, B.; Štrancar, J. Tuning EPR spectral parameters with a genetic algorithm. *Appl. Soft Comput.* **2001**, *1*, 83−90.

(24) Steinhoff, H. J.; Savitsky, A.; Wegener, C.; Pfeiffer, M.; Plato, M.; Möbius, K. High-field EPR studies of the structure and conformational changes of site directed spin labeled bacteriorhodopsin. *Biochim. Biophys. Acta* **2000**, *1457*, 253−262.

(25) Štrancar, J.; Šentjurc, M.; Schara, M. Fast and accurate characterization of biological membranes by EPR spectral simulations of nitroxides. *J. Magn. Reson.* **2000**, *142*, 254−265.

(26) Wickner, W. Asymmetric orientation of a phage coat protein in cytoplasmic membrane of *Escherichia coli*. *Proc. Natl. Acad. Sci. U.S.A.* **1975**, *72*, 4749−4753.

(27) Ohkawa, I.; Webster, R. E. The orientation of the major coat protein of bacteriophage f1 in the cytoplasmic membrane of *Escherichia coli*. *J. Biol. Chem.* **1981**, *256*, 9951−9958.

(28) Fernandes, F.; Loura, L. M.; Prieto, M.; Koehorst, R.; Spruijt, R. B.; Hemminga, M. A. Dependence of M13 major coat protein oligomerization and lateral segregation on bilayer composition. *Biophys. J.* **2003**, *85*, 2430−41.

(29) Subczynski, W. K.; Hyde, J. S. The diffusion-concentration product of oxygen in lipid bilayers using the spin-label T1 method. *Biochim. Biophys. Acta* **1981**, *643*, 283−291.

(30) Subczynski, W. K.; Hyde, J. S. Concentration of oxygen in lipid bilayers using a spin-label method. *Biophys. J.* **1983**, *41*, 283−286.

(31) Subczynski, W. K. Spin-label oximetry in biological and model systems. *Curr. Top. Biophys.* **1999**, *23*, 69−77.

(32) Bogusky, M. J.; Leo, G. C.; Opella, S. J. Comparison of the dynamics of the membrane-bound form of fd coat protein in micelles and in bilayers by solution and solid-state nitrogen-15 nuclear magnetic resonance spectroscopy. *Proteins: Struct., Funct., Genet.* **1988**, *4*, 123−130.

(33) Hemminga, M. A.; Sanders, J. C.; Spruijt, R. B. Spectroscopy of lipid−protein interactions. Structural aspects of two different forms of the coat protein of bacteriophage M13 incorporated in model membranes. In *Progress in Lipid Research*; Sprecher, H., Ed.; Pergamon Press: Oxford, 1992; Vol. 31, pp 301−333.

(34) Leo, G. C.; Colnago, L. A.; Valentine, K. G.; Opella, S. J. Dynamics of fd coat protein in lipid bilayers. *Biochemistry* **1987**, *26*, 854−862.

(35) Marvin, D. A. Filamentous phage structure, infection and assembly. *Curr. Opin. Struct. Biol.* **1998**, *8*, 150−158.

(36) McDonnell, P. A.; Shon, K.; Kim, Y.; Opella, S. J. Fd coat protein structure in membrane environments. *J. Mol. Biol.* **1993**, *233*, 447−463.

(37) Papavoine, C. H. M.; Christiaans, B. E. C.; Folmer, R. H. A.; Konings, R. N. H.; Hilbers, C. W. Solution structure of the M13 major coat protein in detergent micelles; a basis for a model of phage assembly involving specific residues. *J. Mol. Biol.* **1998**, *282*, 401−419.

(38) Spruijt, R. B.; Wolfs, C. J. M.; Hemminga, M. A. Membrane assembly of M13 major coat protein: evidence for a structural adaptation in the hinge region and a tilted transmembrane domain. *Biochemistry* **2004**, *43*, 13972−13980.

(39) Marassi, F. M.; Opella, S. J. Simultaneous assignment and structure determination of a membrane protein from NMR orientational restraints. *Protein Sci.* **2003**, *12*, 403−411.

(40) Papavoine, C. H. M.; Konings, R. N. H.; Hilbers, C. W.; Van de Ven, F. J. M. Location of M13 coat protein in sodium dodecyl sulfate micelles as determined by NMR. *Biochemistry* **1994**, *33*, 12990−12997.

(41) Williams, K. A.; Glibowicka, M.; Li, Z.; Li, H.; Khan, A. R.; Chen, Y. M. Y.; Wang, J.; Marvin, D. A.; Deber, C. M. Packing of coat protein amphipathic and transmembrane helixes in filamentous bacteriophage M13: role of small residues in protein oligomerization. *J. Mol. Biol.* **1995**, *252*, 6−14.

(42) Glaubitz, C.; Grobner, G.; Watts, A. Structural and orientational information of the membrane embedded M13 coat protein by ^{13}C-MAS NMR spectroscopy. *Biochim. Biophys. Acta* **2000**, *1463*, 151−161.

(43) Koehorst, R. B.; Spruijt, R. B.; Vergeldt, F. J.; Hemminga, M. A. Lipid bilayer topology of the transmembrane alpha-helix of M13 Major coat protein and bilayer polarity profile by site-directed fluorescence spectroscopy. *Biophys. J.* **2004**, *87*, 1445−1455.

CI0501490